



## Nano Au-decorated boron nitride nanotubes: Conductance modification and field-emission enhancement

Hua Chen, Hongzhou Zhang, Lan Fu, Ying Chen, James S. Williams, Chao Yu, and Dapeng Yu

Citation: [Applied Physics Letters](#) **92**, 243105 (2008); doi: 10.1063/1.2943653

View online: <http://dx.doi.org/10.1063/1.2943653>

View Table of Contents: <http://scitation.aip.org/content/aip/journal/apl/92/24?ver=pdfcov>

Published by the [AIP Publishing](#)

---

### Articles you may be interested in

[Field emission characteristics from graphene on hexagonal boron nitride](#)

Appl. Phys. Lett. **104**, 221603 (2014); 10.1063/1.4881718

[Excellent oxidation endurance of boron nitride nanotube field electron emitters](#)

Appl. Phys. Lett. **104**, 163102 (2014); 10.1063/1.4870655

[Electronic and field emission properties of boron nitride/carbon nanotube superlattices](#)

Appl. Phys. Lett. **81**, 46 (2002); 10.1063/1.1491013

[Field emission characteristics of boron nitride films deposited on Si substrates with cubic boron nitride crystal grains](#)


J. Vac. Sci. Technol. B **19**, 1051 (2001); 10.1116/1.1361042

[Synthesis and field-emission behavior of highly oriented boron carbonitride nanofibers](#)

Appl. Phys. Lett. **76**, 2624 (2000); 10.1063/1.126429


---

Agilent's Electronic Measurement Group is becoming **Keysight Technologies**.



**Engineering Education & Research Resources DVD 2014**

Agilent is the key to your test and measurement needs **Order yours**

The advertisement features a row of colorful icons representing various engineering and research fields: a green Wi-Fi symbol, a blue checkmark, a blue graduation cap, a green book, a yellow sun, a green network diagram, a blue antenna, a purple microchip, a green wave, an orange vertical bar, and a red starburst. The Agilent Technologies logo is positioned at the bottom center of the advertisement.

## Nano Au-decorated boron nitride nanotubes: Conductance modification and field-emission enhancement

Hua Chen,<sup>1,a)</sup> Hongzhou Zhang,<sup>1</sup> Lan Fu,<sup>1</sup> Ying Chen,<sup>1</sup> James S. Williams,<sup>1</sup> Chao Yu,<sup>2</sup> and Dapeng Yu<sup>2</sup>

<sup>1</sup>Research School of Physical Sciences and Engineering, The Australian National University, Australian Capital Territory 0200, Australia

<sup>2</sup>Electron Microscopy Laboratory and State Key Laboratory for Mesoscopic Physics, School of Physics, Peking University, Beijing 100871, People's Republic of China

(Received 3 March 2008; accepted 14 May 2008; published online 17 June 2008)

This letter reports the electrical and field-emission properties of Au-decorated boron nitride nanotubes (Au-BNNTs). The insulating BNNTs become metallic after Au coating as the Au coverage exceeds a critical value. The Au decoration modifies the work function of the BNNTs and, as a consequence, the field-emission current densities of Au-BNNTs are significantly enhanced. Correspondingly, the turn-on field of the Au-BNNTs is reduced to one third and the emission current density is increased by four orders in contrast to pure BNNTs. The experimental results demonstrate that such Au-BNNTs are promising electron field emitters. © 2008 American Institute of Physics. [DOI: 10.1063/1.2943653]

Studies on the boron nitride (BN) thin films,<sup>1,2</sup> nanotubes,<sup>3</sup> nanorods,<sup>4</sup> and BN coated Si tip<sup>5</sup> have already demonstrated their stable and reliable field-emission characteristics. The BN nanotubes (BNNTs) are very promising as field emitters because they combine the increase of the field-enhancement factor caused by the tubular shape with the surface negative electron affinity (NEA).<sup>6,7</sup> In conjunction with high mechanical strength,<sup>8</sup> chemical stability,<sup>9</sup> oxidation resistance,<sup>9</sup> and excellent thermal conductivity,<sup>10</sup> BNNTs are expected to have the prospective application in flat panel displays. Nonetheless, a good electrical insulating property determines the low field-emission current density of pure BNNTs in contrast to that of carbon nanotubes (CNTs).<sup>11</sup> Therefore, further modifications in BNNTs are necessary to improve their field-emission property. For instance, carbon doping of BNNTs has been illustrated in the prospect to lower the turn-on fields and to subsequently increase the field-emission current densities.<sup>12</sup> In this letter, we propose using nanogold (Au) to decorate the surface of BNNTs in an attempt for modifying the electrical property and associated field-emission feature.

The BNNTs were synthesized using a ball milling and annealing method.<sup>13,14</sup> In this procedure, amorphous boron powder was first loaded into a stainless steel planetary mill with steel balls ( $\Phi 25.4$  mm AISI 420) under  $\text{NH}_3$  atmosphere for ball milling treatment. The catalytic particles [iron]<sup>15</sup> were produced and mixed with boron powder in the milling process, and the content of iron particles was controlled below 1.5 at % by adjusting the milling parameters. The milled powder was then annealed at 1100 °C in a quartz tube furnace in a  $\text{N}_2$  flow of 100 ml/min. After 15 h of annealing, a large percentage of powder was transformed into long BNNTs.

A dc magnetron sputter (Emitech K575X) was used to create nano-Au spots on the surface of BNNTs. The sputtering was carried out in Ar atmosphere (4 Pa). The sputtering current was 5 mA. The conductance of individual Au-

BNNTs was measured using the two-points configuration. A single nanotube was affixed on Ni electrodes using Silver paste (DuPont) and an ohmic contact was achieved after heating the sample at 400 °C in the air for 10 min. *I-V* characteristics of nanotubes were then measured utilizing a pico-ampere meter/dc voltage source (HP 4140B). To investigate their field-emission properties, BNNTs were randomly disposed on a Si substrate as the cathode and a metal plate was utilized as the anode. The distance between the sample and the anode was 100  $\mu\text{m}$  and the measurement was carried out in a vacuum chamber with an ultimate pressure of  $5 \times 10^{-7}$  Pa. The emission current was measured by a Keithley 485 picoameter.

Figure 1(a) is a scanning electron microscopy (SEM) (Hitachi 4500) image exhibiting the typical morphology of BNNTs on a Si substrate where the BNNTs possess an average diameter of 130 nm. With the help of a high resolution transmission electron microscopy (TEM) (Philips CM300), a bamboolike structural feature is observed and the image is displayed in Fig. 1(b). The interplanar spacing of 0.34 nm obtained from Fig. 1(c) is identical to the distance of hexagonal BN (002) basal planes. The energy dispersive spectrometer (EDS) identifies that the ratio of B/N of the nano-

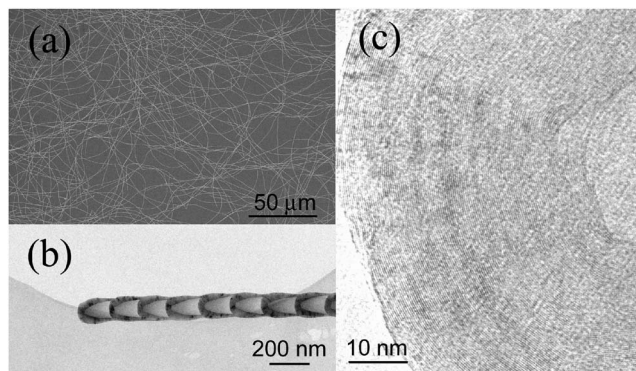


FIG. 1. BN nanotubes. (a) SEM image shows high purity BNNTs. (b) TEM image shows a bamboolike structure feature. (c) High resolution TEM image shows that the interplanar spacing is 0.34 nm.

<sup>a)</sup>Electronic mail: hua.chen@anu.edu.au.

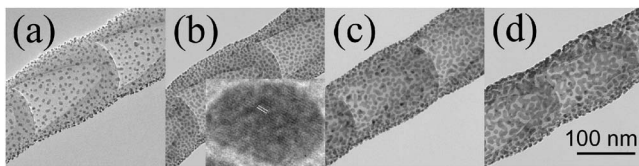


FIG. 2. TEM images of Au-BNNTs under different sputtering times. (a) Small Au spots are obtained at 20 s. (b) The size of the Au spots increases at 40 s; inset TEM image shows a Au spot with the interplanar spacing of 0.24 nm which refers to Au (111) planes. (c) some Au-spots combine together to form Au islands at 80 s. (d) Au islands are connected to form quasicontinuous Au coating at 120 s.

tube is around 1. Figure 2 shows the TEM images of Au-decorated BNNTs with different sputtering times of 20, 40, 80 and 120 s, referring to Au20, Au40, Au80, and Au120, respectively. The Au spots of Au20 are separated from each other as shown in Fig. 2(a). Compared with Au20, longer coating time produces larger isolating Au spots on Au40 [see Fig. 2(b)]. The adjacent Au spots of Au80 start to connect and form islands, as revealed in Fig. 2(c). As the sputtering time further increased, the dimensions of Au islands expand and many of them are interlinked [see Fig. 2(d)]. The inset in Fig. 2(b) shows that the interplanar spacing of an Au spot is approximately 0.24 nm which is identical to the interplanar spacing of Au (111) planes.

According to the conventional percolation theory<sup>16</sup>, the conductance of Au-decorated BNNTs is expected to deviate from that of pure BNNTs. Figure 3 shows the conductance of Au-decorated BNNTs ( $\Omega^{-1}$ ) with respect to the sputtering time (seconds). As indicated by the solid curves in Fig. 3, with the sputtering time less than 120 s, the relationship between the conductance and the sputtering time can be fitted perfectly with an exponential function. However, if the sputtering time is beyond 120 s, the conductance linearly increases with the sputtering time. Figure 4 shows  $I$ - $V$  features of Au40, Au80, and Au120 in conductance measurements. The linear relationship suggests Ohmic contact between the single nanotube and electrodes for all of samples. The TEM analyses demonstrated that the longer the sputtering time, the higher the Au coverage on the surface of BNNTs [see Fig. 2]. In addition, a quasicontinuous Au layer forms as the sputtering time exceeds 120 s. Consequently, the metallic conductance of the surface Au layer becomes dominant. Therefore, after the formation of a continuous Au layer, increasing the sputtering time further results in a linear raise in conductance, as shown in Fig. 3. However, from the percolation theory,<sup>17</sup> if the Au coverage fell below a critical fraction the conductance of the Au-decorated BNNTs (Au20, Au40, and Au80) would be strongly dependent on that of the pure BNNTs. The sputtering time to obtain the coverage with the critical fraction should be around 105 s according to the same theory.

The field-emission properties of the pure and Au-decorated BNNTs (Au40 and Au80) were studied as the present work concerned the electron field emission of Au-BNNTs instead of a continuous Au film. Figure 5 represents the emission current density ( $J$ ) of the pure and Au-decorated BNNTs as a function of the macroscopic electrical field ( $E_{\text{mac}}$ ) applied on samples,  $E_{\text{mac}} = V/d$ , where  $V$  and  $d$  are the cathode-anode voltage and distance, respectively. The turn-on fields of pure BNNTs, Au40 and Au80, which are arbitrarily defined as the electrical field resulting in an emis-

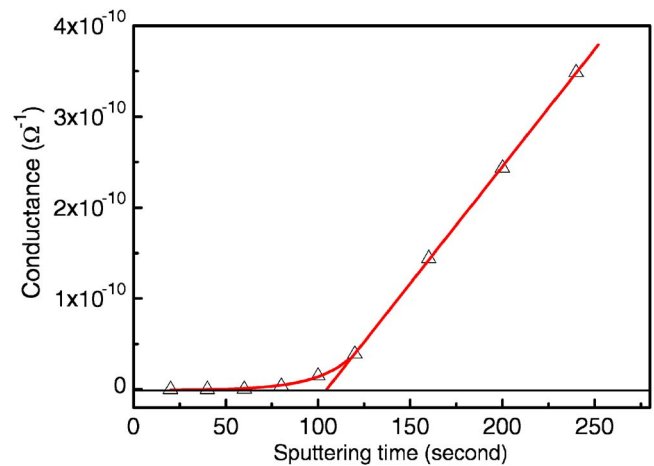


FIG. 3. (Color online) Conductance of the Au-BNNTs with respect to different sputtering times. After 120 s, there is a linear relationship between the conductance and sputtering time.

sion current density of 10 nA/cm<sup>2</sup>, are 18, 11, and 3.9 V/ $\mu$ m, respectively. It is clear that the Au decoration can significantly decrease the turn-on field of the BNNT emitters. In addition, under the same macroscopic electrical field, the field-emission current density of Au40 increases about two orders in comparison with that of pure BNNTs. Similarly, the emission current density of Au80 is about two orders higher than that of Au40. These results suggest that the field-emission properties of BNNTs can be dramatically improved by Au decoration.

Fowler–Nordheim (FN) theory<sup>18</sup> has been widely practiced to illustrate the mechanism of electron field emission. It describes the electron tunneling through an interface barrier. In the FN model, the field-emission current density ( $J$ ) of the emitter is expressed as a function of the tip work function ( $\Phi$ ) and the local electrical field at the emitter surface ( $E_{\text{loc}}$ ),<sup>19</sup>

$$J \propto E_{\text{loc}}^2 \exp(-6.8 \times 10^{10} \Phi^{3/2} / E_{\text{loc}}), \quad (1)$$

where  $E_{\text{loc}}$  has a unit of V/ $\mu$ m,  $\Phi$  has a unit of eV, and  $J$  has a unit of A/cm<sup>2</sup>. Marcus *et al.*<sup>20</sup> constructed a relationship between  $E_{\text{mac}}$  and  $E_{\text{loc}}$  for an emitter of hemispherical morphology. When the distance between the emitter and the an-

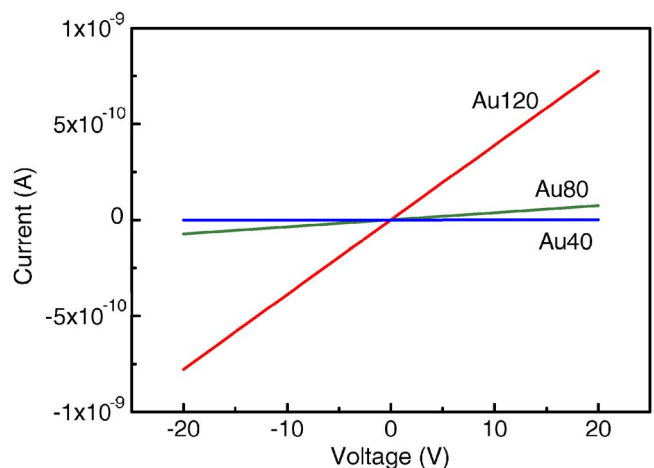


FIG. 4. (Color online)  $I$ - $V$  features of Au40, Au80, and Au120. The linear relationship suggests Ohmic contact between the single nanotube and electrodes for all of samples.

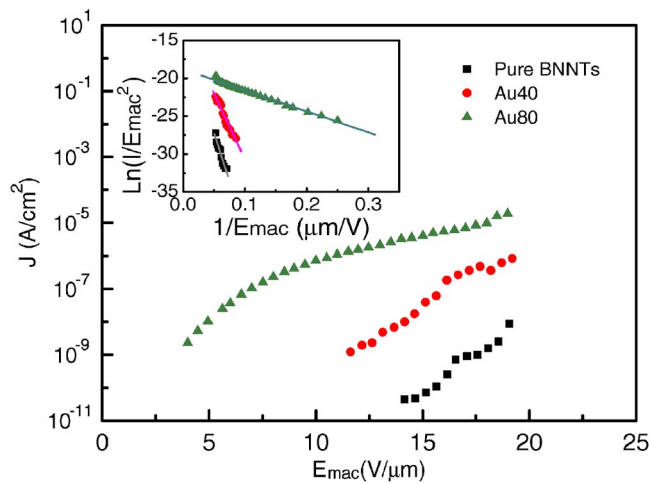


FIG. 5. (Color online) Emission current densities of pure and Au-decorated BNNTs as a function of  $E_{\text{mac}}$ . The emission current density of the pure BNNTs is unsaturated at high field. The emission current density of Au40 increases by almost two orders, and it remains in the unsaturated state under the same macroscopic electrical field. For Au80, the current density saturation appears at the high electrical field range. The inset shows corresponding FN plots in which the Au80 has a significant variation in the slope.

ode  $d$  is much greater than the radius of the emitter tip ( $r_{\text{tip}}$ ),  $E_{\text{loc}}$  is reciprocally proportional to  $r_{\text{tip}}$ , ( $E_{\text{loc}} = V/r_{\text{tip}}$ ). A factor  $\alpha$  ( $\geq 1$ ) is introduced where  $d \gg r_{\text{tip}}$  is ungratified. In this case,  $E_{\text{loc}}$  could be expressed as

$$E_{\text{loc}} = V/(\alpha r_{\text{tip}}) = d/\alpha r_{\text{tip}} \times E_{\text{mac}}. \quad (2)$$

Modifying Eq. (1) by introducing Eq. (2) and changing current density  $J$  to current  $I$ , the FN equation can be expressed as

$$\ln(I/E_{\text{mac}}^2) = (1/E_{\text{mac}})[-6.8 \times 10^{10}(\alpha r_{\text{tip}}/d)\Phi^{3/2}] + \text{offset}. \quad (3)$$

The above equation predicts a linear relation between  $\ln(I/E_{\text{mac}}^2)$  and  $1/E_{\text{mac}}$ , i.e., FN plot. For our particular configuration and measurement condition,  $r_{\text{tip}}$  and  $d$  are ensemble averages of randomly oriented BNNTs.<sup>4</sup> Because of the large quantity of nanotubes and the high uniformity of their morphology, it can be safely assumed that the values of  $r_{\text{tip}}$  and  $d$  of the measured samples are very close to each other. Hence, variations in the work function of samples are evaluated through the slopes  $S_{\text{FN}}$  of FN plots.  $S_{\text{FN}} = -6.8 \times 10^{10}(\alpha r_{\text{tip}}/d)\Phi^{3/2} = -A\Phi^{3/2}$ ,  $A$  is a geometric factor and keeps constant for all our samples. The inset of Fig. 5 is the FN plots of our samples. We first use the work function  $\Phi$  ( $\sim 6$  eV) and the  $S_{\text{FN}}$  of pure BNNTs to acquire the constant  $A$ . Then, the work functions  $\Phi$  of Au40 and Au80 are estimated to be 4.8 and 1.4 eV. The work function of Au40 approaches the value of pure gold (4.8 eV).<sup>21</sup> For Au80, the smaller work function suggests formation of a much smaller surface barrier. This indicates that Au possibly diffused into the BNNTs during the deposition so that a surface of NEA might be formed in Au80 as observed on the Au–Al<sub>2</sub>O<sub>3</sub> interface.<sup>22</sup> However, a detailed investigation is required to further clarify the mechanism of the dramatic decrease of the work function of Au80. Nevertheless, the results collected suggest that nano Au decoration can significantly improve

the field-emission characteristics of BNNTs by decreasing the work function.

Unlike the field emission of CNTs, where the current saturation happens under high electrical fields ( $> \sim 5$  V/ $\mu\text{m}$ ),<sup>23</sup> the emission current density of pure BNNTs does not saturate even at the much higher electrical field [see Fig. 5]. For CNTs' emitter, Zhong *et al.*<sup>24</sup> addressed that the current saturation occurred at a large emission current because contact resistance of the substrate and CNTs obstructed the supplement of electrons to the emitting sites. The current saturation of Au80 may arise from a similar mechanism because the conductance is increased to some value by Au coating.

In conclusion, the conductance of Au-BNNTs is increased with respect to the sputtering time. The Au decoration modifies the work function of the BNNTs and, as a consequence, the field-emission current densities of Au-BNNTs are significantly enhanced. Correspondingly, the turn-on field of such Au-BNNTs is reduced to one third and the emission current density is increased by four orders in contrast to pure BNNTs.

The authors acknowledge the financial support from the Australian Research Council, and technical support from staffs of the Electron Microscopy Unit at the Australian National University.

<sup>1</sup>T. Sugino, C. Kimura, T. Yamamoto, and S. Funakawa, *Diamond Relat. Mater.* **12**, 464 (2003).

<sup>2</sup>H. Luo, S. Funakawa, W. Shen, and T. Sugino, *J. Vac. Sci. Technol. B* **22**, 1958 (2004).

<sup>3</sup>J. Cumings and A. Zettl, *Solid State Commun.* **129**, 661 (2004).

<sup>4</sup>H. Z. Zhang, Q. Zhao, J. Yu, D. P. Yu, and Y. Chen, *J. Phys. D* **40**, 144 (2007).

<sup>5</sup>T. Sugino, S. Kawasaki, K. Tanioka, and J. Shirafuji, *Appl. Phys. Lett.* **71**, 2704 (1997).

<sup>6</sup>M. J. Powers, M. C. Benjamin, L. M. Porter, R. J. Nemanich, R. F. Davis, J. J. Cuomo, G. L. Doll, and S. J. Harris, *Appl. Phys. Lett.* **67**, 3912 (1995).

<sup>7</sup>K. P. Loh, I. Sakaguchi, M. N. Gamo, S. Tagawa, T. Sugino, and T. Ando, *Appl. Phys. Lett.* **74**, 28 (1999).

<sup>8</sup>N. G. Chopra and A. Zettl, *Solid State Commun.* **105**, 297 (1998).

<sup>9</sup>Y. Chen, J. Zou, S. J. Campbell, and G. L. Caer, *Appl. Phys. Lett.* **84**, 2430 (2004).

<sup>10</sup>C. W. Chang, W.-Q. Han, and A. Zettl, *Appl. Phys. Lett.* **86**, 173102 (2005).

<sup>11</sup>D. Golberg, Y. Bando, C. Tang, and C. Zhi, *Adv. Mater. (Weinheim, Ger.)* **19**, 2413 (2007).

<sup>12</sup>H. Y. Zhu, D. J. Klein, N. H. March, and A. Rubio, *J. Phys. Chem. Solids* **59**, 1303 (1998).

<sup>13</sup>Y. Chen, J. Fitz Gerald, J. S. Williams, and S. Bulcock, *Chem. Phys. Lett.* **299**, 260 (1999).

<sup>14</sup>Y. Chen, M. Conway, J. S. Williams, and J. Zou, *J. Mater. Res.* **17**, 1896 (2002).

<sup>15</sup>L. T. Chadderton and Y. Chen, *J. Cryst. Growth* **240**, 164 (2002).

<sup>16</sup>B. J. Last and D. J. Thouless, *Phys. Rev. Lett.* **27**, 1719 (1971).

<sup>17</sup>M. F. Sykes and J. W. Essam, *Phys. Rev.* **133**, A310 (1964).

<sup>18</sup>R. H. Fowler and L. Nordheim, *Proc. R. Soc. London, Ser. A* **119**, 173 (1928).

<sup>19</sup>P. G. Collins and A. Zettl, *Phys. Rev. B* **55**, 9391 (1997).

<sup>20</sup>R. B. Marcus, K. K. Chin, Y. Yuan, H. Wang, and W. N. Carr, *IEEE Trans. Electron Devices* **37**, 1545 (1990).

<sup>21</sup>P. A. Anderson, *Phys. Rev.* **115**, 553 (1959).

<sup>22</sup>R. Banan-Sadeghian, S. Badilescu, Y. Djaoued, S. Balaji, V. Truong, and M. Kahrizi, *IEEE Electron Device Lett.* **29**, 312 (2008).

<sup>23</sup>C. Klinke, E. Delvigne, J. V. Barth, and K. Kern, *J. Phys. Chem. B* **109**, 21677 (2005).

<sup>24</sup>D. Y. Zhong, G. Y. Zhang, S. Liu, T. Sakurai, and E. G. Wang, *Appl. Phys. Lett.* **80**, 506 (2002).